NAOS-CONICA Performance in a Crowded Field – the Arches Cluster

A. STOLTE[1], W. BRANDNER[1], E.K. GREBEL[1], DON F. FIGER[2], F. EISENHAUER[3], R. LENZEN[1], Y. HARAYAMA[3]

[1]*Max-Planck-Institut für Astronomie, Heidelberg, Germany*
[2]*Space Telescope Science Institute, Baltimore, USA*
[3]*Max-Planck-Institut für Extraterrestrische Physik, Garching, Germany*

1. NAOS-CONICA – Near-Infrared Camera with Adaptive Optics

NAOS-CONICA is a near-infrared imaging camera and spectrograph (CONICA) attached to an adaptive optics (AO) system (NAOS) for wavefront corrections (Lenzen et al. 1998, Rousset et al. 2000). The AO system is designed to deliver diffraction-limited observations at an 8-metre-class telescope. NAOS is equipped with two Shack-Hartmann wavefront sensors operating at visual and NIR wavelengths, respectively. Most existing AO systems feed near-infrared (NIR) cameras, but operate at visual wavelengths. In addition to the fact that the spectral energy distribution of bright stars peaks at optical wavelengths, visual detectors offer higher sensitivity and lower read-out noise than NIR detectors, thus allowing one to use fainter targets for wavefront sensing. The restriction to visual reference sources, however, excludes deeply embedded objects located in regions with active star formation or high foreground extinction such as the Galactic Centre. With wavefront sensors operating both at visual and NIR wavelengths, NAOS combines the advantages of visual, faint reference targets with the option to penetrate highly obscured regions containing bright infrared sources. NAOS-CONICA was commissioned on Yepun (UT4) in the course of Period 69. For more detailed information on NACO performance and first light, see Brandner et al. (2002) in *The Messenger* 107.

We have used the CONICA *JHK* imaging mode with the S27 camera in combination with the NAOS visual wavefront sensor for performance tests in the crowded stellar field of the dense, massive star cluster Arches. The S27 camera with a pixel scale of 27 milliarcsecond (mas) and corresponding field of view (FOV) of 27″ × 27″ is optimized for diffraction-limited observations in the *J* to *K* band wavelength range. At 2.2 μm, the diffraction limit of an 8-m telescope is 57 mas, such that the S27 camera allows Nyquist sampling.

2. Why Arches?

The Arches cluster is one of the few starburst clusters found in the Milky Way. With an age of only ~ 2–3 Myr it contains a rich massive stellar population with about 150 O stars located in the cluster centre (Figer et al. 1999), and several more found in the immediate vicinity. The core density has been estimated to be $3 \cdot 10^5$ $M_\odot$ pc^{-3}, and the total stellar mass exceeds 10^4 $M_\odot$ (Figer et al. 1999). The massive cluster centre contains ~ 12 Wolf-Rayet stars (Cotera et al. 1996, see also Blum et al. 2001), intertwined with an intermediate-mass main-sequence population. At the faint end, where pre-main-sequence stars would be expected, the stellar population is severely contaminated by bulge stars, as Arches is located in the central region of the Milky Way at a projected distance of only 25 pc (roughly 10 arcminutes) from the Galactic Centre (Fig. 1).

With a distance of about 8 kpc and a foreground extinction in the visual of 24 to 34 mag, Arches is a very challenging object. The high foreground extinction obscures the faint cluster population at visual wavelengths, so that NIR observations, where extinction is less severe, are necessary to detect the cluster population. Given these extreme properties, and the existence of data sets obtained with HST/NICMOS and the Gemini/ Hokupa'a AO system allowing a detailed comparison, the Arches cluster was chosen as NAOS-CONICA commissioning target to test the NACO performance on a dense, crowding-limited stellar field.

3. NAOS-CONICA Commissioning Data

Arches *H* and K_s images were obtained during Commissioning 3 of NAOS-CONICA in March and April 2002. 20 exposures with integration times of 1 min (2 × 30 s detector integration time (DIT)) each were obtained in *H*, and 15 × 1 min exposures in K_s (4 × 15 s DIT). As the NIR wavefront sensor was not available during Comm 3, a blue foreground giant with V = 16 mag ($V-R$ ~1 mag) served as the reference source for the visual wavefront sensor. Although the brightest star in the Arches field, this star is already close to the limiting magnitude (~17 mag) of the visual wavefront sensor. As has been demonstrated on the Galactic Centre field (Schödel et al. 2002 and Ott et al. in this issue), NIR wavefront sensing with NIR bright reference targets (K ~10 mag) is capable of improving the performance in a highly extincted region.

All images were taken in auto-jitter mode. The auto-jitter template allows automatic, random offsets between individual exposures to facilitate background subtraction and avoid afterglows at the position of bright sources. A set of additional exposures with short detector integration times were taken to obtain photometry of the bright cluster stars (8 × 1 s DIT in *H*, 8 × 0.5 s DIT in K_s). Seeing conditions varied during the Arches observations. In *H*-band, the seeing ranged from 0.45 to 0.85, while during *K*-band observations the seeing degraded from 0.8 to 1.3. On April 4, the moon was only 6° from our target, and increased background fluctuations decreased the detectability of faint sources in the cluster vicinity.

The data were reduced within IRAF, using twilight flat fields taken during Comm 3 and combined with the nacop twflat algorithm in *eclipse* (Devillard 1997). *Eclipse* is the ESO pipeline reduction package, which allows special treatment of particular instrument characteristics adapted to the available ESO instrumentation. Sky frames were created from the cluster observations themselves, which is not ideal, but was sufficient for our technical study. Starlight was excluded from these skies by rejecting the bulk of the bright pixels. As the CONICA detector has a significant fraction of time-varying hot pixels, a cosmic ray rejection routine was used to obtain a bad pixel mask. This mask was applied during the drizzling process, in which images are shifted and combined. The 7 exposures with the highest resolution were combined in K_s to one 7 min integrated frame, and the 14 best exposures in *H*, where seeing conditions were much more stable, could be used to obtain a 14 min *H*-band image. During the *K*-band observations, the AO performance changed with time as the seeing worsened. As crowding is the limiting factor on the Arches field, the gain in resolution by rejecting the large fraction of frames with lower quality supersedes the loss in photometric depth due to the shorter resulting total integration time on the fi-

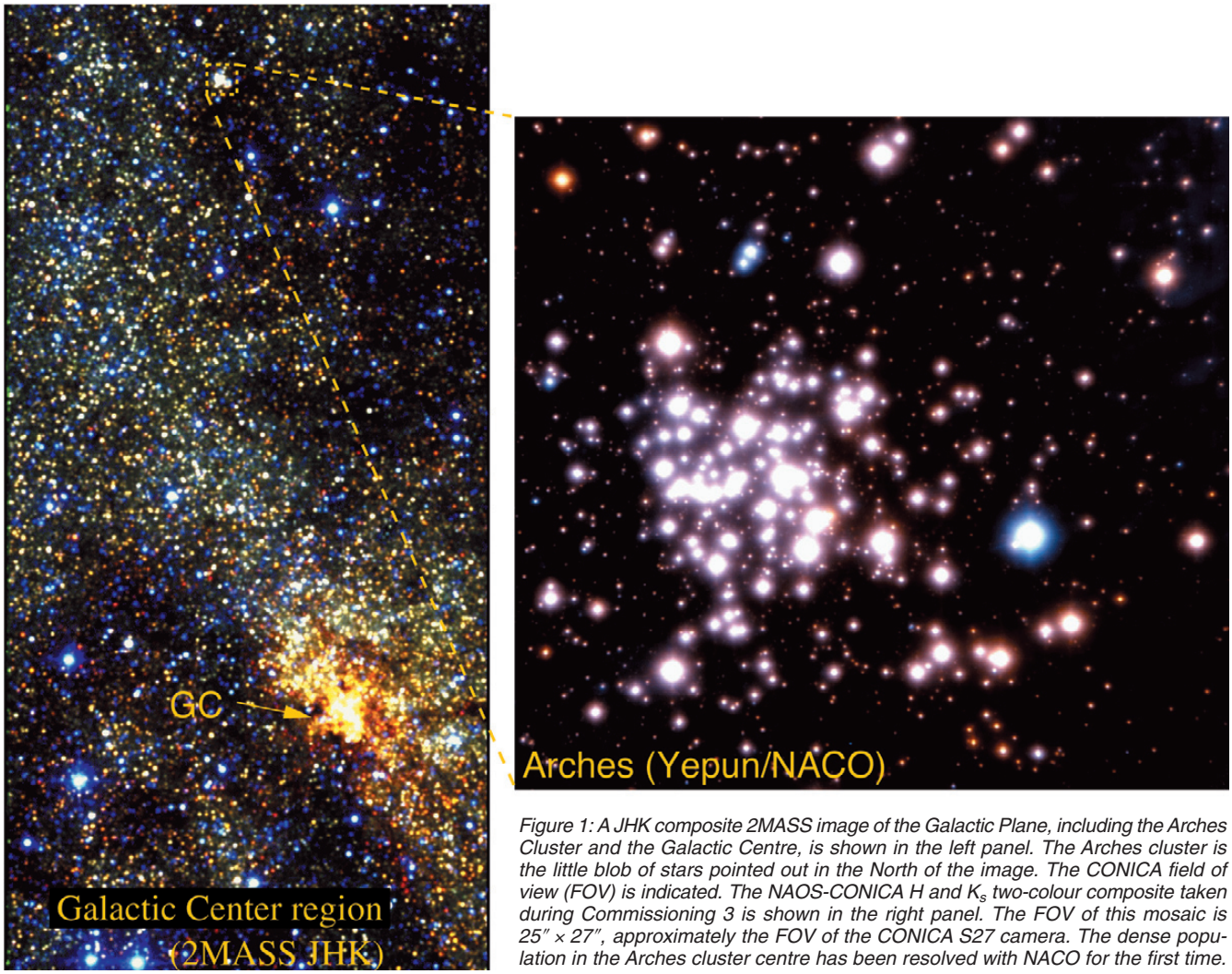

Figure 1: A JHK composite 2MASS image of the Galactic Plane, including the Arches Cluster and the Galactic Centre, is shown in the left panel. The Arches cluster is the little blob of stars pointed out in the North of the image. The CONICA field of view (FOV) is indicated. The NAOS-CONICA H and K_s two-colour composite taken during Commissioning 3 is shown in the right panel. The FOV of this mosaic is 25″ × 27″, approximately the FOV of the CONICA S27 camera. The dense population in the Arches cluster centre has been resolved with NACO for the first time.

nal image (see also Tessier et al. 1994). The best *K*-band photometry was obtained when combining only the frames where the best AO performance was achieved. The resulting images have Strehl ratios of 14% in *H* and 20 % in *K*, yielding a spatial resolution of ~ 85 mas in both filters.

Standard DAOPHOT PSF fitting photometry was used to obtain the final magnitudes. A constant PSF function has been used, as isolated PSF stars are rare in the dense Arches field. A Penny function, which has a Gaussian core with elongated Lorentzian wings, yielded the best fit to the data.

The NACO data were calibrated using existing HST/NICMOS photometry of the same field (Figer et al. 1999). All calibrated data shown below are in the NICMOS photometric system. This allowed a large number of stars to be used for zero-pointing and for the study of photometric residuals over the field. We find the NACO performance to be very stable over the field. No trend of the amplitude of photometric residuals with field position is observed. Note that the measurement of anisoplanatism on the Arches field is complicated by the high stellar density and large density gradient over small spatial scales.

4. Luminosity Functions

In Figure 2, luminosity functions (LFs) of the NACO commissioning data are compared to HST/NICMOS LFs of the same field. Arches was observed with NICMOS2 for 256 s integration time in the broadband filters F110W, F160W and F205W corresponding to *J*, *H*, and *K*. The NICMOS detection limits were approximately 21 mag in *H* (F160W), and 20 mag in *K* (F205W). Within a factor of 2 longer integration time in *K* and a factor of 3.3 in *H*, NACO reaches detection limits of 22 mag in *H* and 21 mag in *K*, one magnitude deeper than the NICMOS observations. Note that NICMOS does not have to fight the large NIR background from the Earth's atmosphere, but also has the much smaller collecting area of a 2.4-m mirror as opposed to Yepun's 8-m mirror.

Only objects detected in both filters are included in the NACO LF, as the requirement that objects have to be detected in both filters is a very efficient method to reject artefacts. In particular in a very dense stellar field, background fluctuations and saturation peaks frequently cause false detections.

As sources in the Arches cluster are hidden behind ~ 30 mag of foreground extinction, reddening influences the detection of stars more severely at shorter wavelengths. Consequently, the *H*-band LF shown in Fig. 2 represents the photometric performance more realistically, as the *K*-band LF is artificially truncated by the requirement that sources have to be detected in *H* as well.

While the field star LF is comparable for NACO and NICMOS down to the NICMOS detection limit of *H* ~ 21 mag, NACO clearly gains a large number of sources in the cluster centre. Here, the significantly better resolution of 85 mas with VLT/NACO vs. 210 mas with HST/NICMOS allows us to resolve the cluster centre for the first time. Note that the diffraction limit of the 2.4 m HST mirror of 183 mas in *H* and 210 mas in *K* does not allow a much higher resolution with NICMOS, while better Strehl ratios may yield resolutions down to the VLT diffraction limit of 57 mas in *H* and 69 mas in *K* with NAOS-CONICA. The cluster centre LF dem-

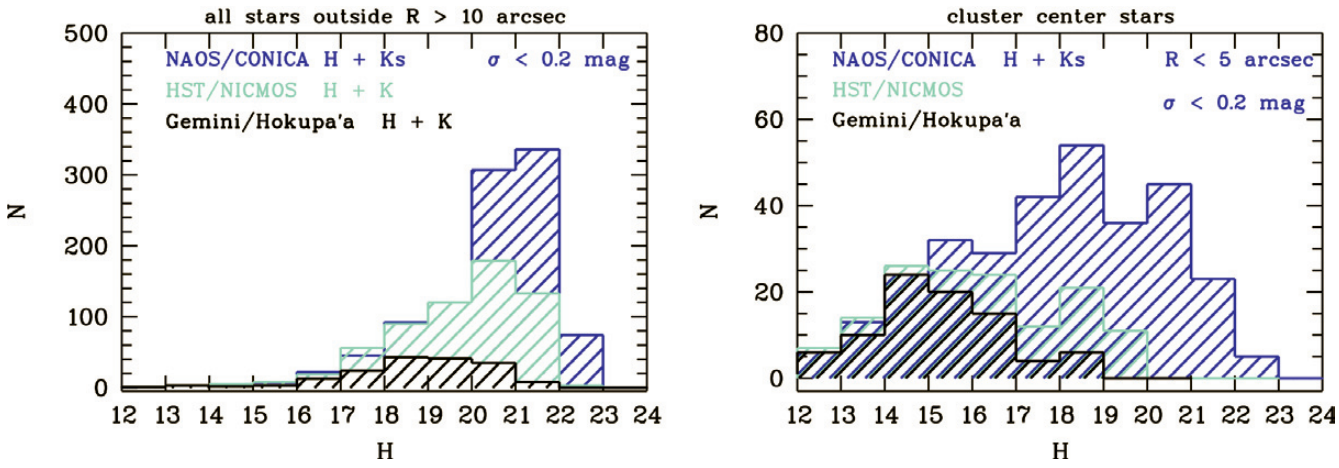

Figure 2: H-band luminosity function of the Arches cluster. The left LF contains only objects at a distance R > 10″ from the cluster centre, displaying the field performance in comparison to HST/NICMOS, while the right panel shows the cluster centre regions with stars within R < 5″. While the field performance between NACO and NICMOS is comparable until the NICMOS detection limit of H ~ 21 mag is approached, the cluster centre LF shows the large gain in the NACO data due to the higher spatial resolution. It is particularly intriguing that already bins fainter than H = 15 mag are affected. This indicates that the cluster centre population was until now never truly resolved, not even at the brighter end.

onstrates not only the deeper photometry with NACO, but also the strongly enhanced resolution, as in nearly each magnitude bin above $H = 15$ mag more stars are resolved. This affects statistically derived properties of the Arches stellar population, such as stellar density, total mass and the slope of the mass function.

5. Colour-Magnitude Diagrams

A comparison of colour-magnitude diagrams (CMDs) of the Arches cluster centre is shown in Figure 3. Here, Gemini/Hokupa'a low Strehl data (2.5% in *H*, 7% in *K*, Stolte et al. 2002), HST/NICMOS observations (Figer et al. 1999), and the new NACO observations are compared. The Gemini data cover the smallest field of view, and care was taken to select only the area in common to all data sets to allow direct comparison. The NACO and NICMOS data were selected accordingly.

While the low-Strehl Hokupa'a data show a large scatter in the main sequence due to the contamination of stellar fluxes with extended seeing halos, the NACO data show a well-confined, narrow main sequence. The NICMOS data are also very well confined, but in accordance with the results from luminosity functions the NACO main sequence appears more densely populated. Derived physical and statistical properties of the cluster population are consequently less biased by crowding losses.

The Hokupa'a data set has the highest incompleteness, being 90% complete only down to $K = 15$ mag. When the number of stars down to this magnitude limit is compared, we find 131 stars with Hokupa'a, 157 stars with NICMOS within the same field, and 169 stars with NACO. The 12 stars undetected with NICMOS are either fainter neighbours vanishing in the PSF pattern of a bright star, or close pairs where only one component has been resolved. Figure 4 shows the comparison of resolved sources with $K < 15$ mag on a sample field in the cluster centre.

6. Mass Function

The NACO CMD was used to derive the mass function (MF) of the Arches cluster population. A 2 Myr isochrone with twice solar metallicity (see Figer et al. 1999, Stolte et al. 2002 for discussion) from the Geneva set of models (Lejeune & Schaerer 2001) was used to transform *K*-band magnitudes into stellar masses.[1] A distance modulus of 14.52 mag and extinction of $A_V = 24$ mag, corresponding to the cluster centre, have been applied. Magnitudes

[1]Note that the current best age estimate from high-resolution spectra of the bright Arches main sequence O stars is 2.5 Myr (Figer et al. 2002), but we prefer to use the 2 Myr isochrone to allow direct comparison of the NACO MF with our prior results given in Figer et al. 1999 and Stolte et al. 2002.

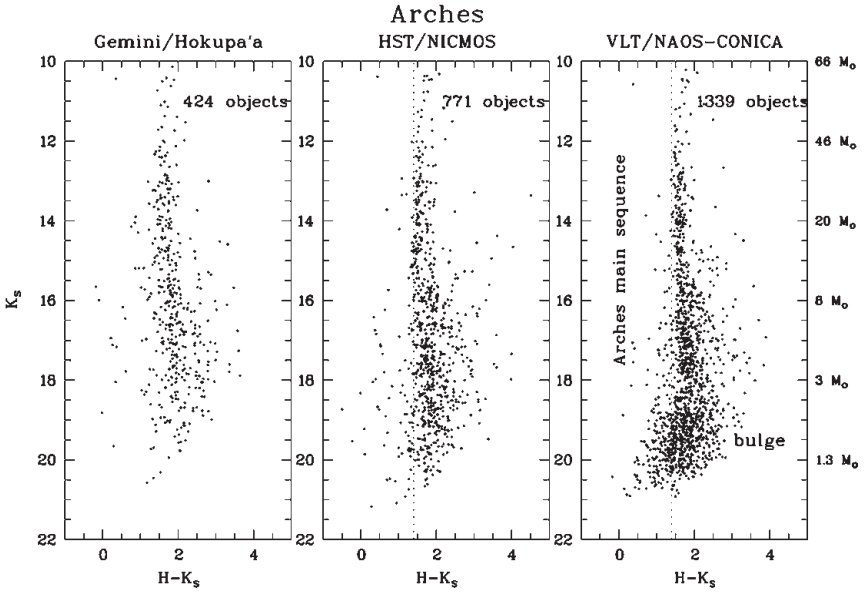

Figure 3: Arches colour-magnitude diagrams. A comparison between VLT/NAOS-CONICA, HST/NICMOS and Gemini/Hokupa'a data is shown. While the low Strehl ratio of the Hokupa'a data of only a few per cent severely limits resolving the cluster population and caused large photometric uncertainties, the moderate Strehl NAOS-CONICA observations exhibit a narrow, well-defined main sequence, reflecting the photometric quality of the data. The NICMOS data are limited by the small telescope diameter of only 2.4 m, and corresponding larger diffraction limit. In addition, the strong diffraction pattern in the NICMOS PSF hampers the detection of faint sources in the cluster centre. Despite the moderate Strehl ratio, the NACO CMD clearly displays the advantages of AO at an 8-m-class telescope. The right axis of the NACO CMD is labelled with present-day masses from a 2 Myr main sequence isochrone used to derive the mass function.

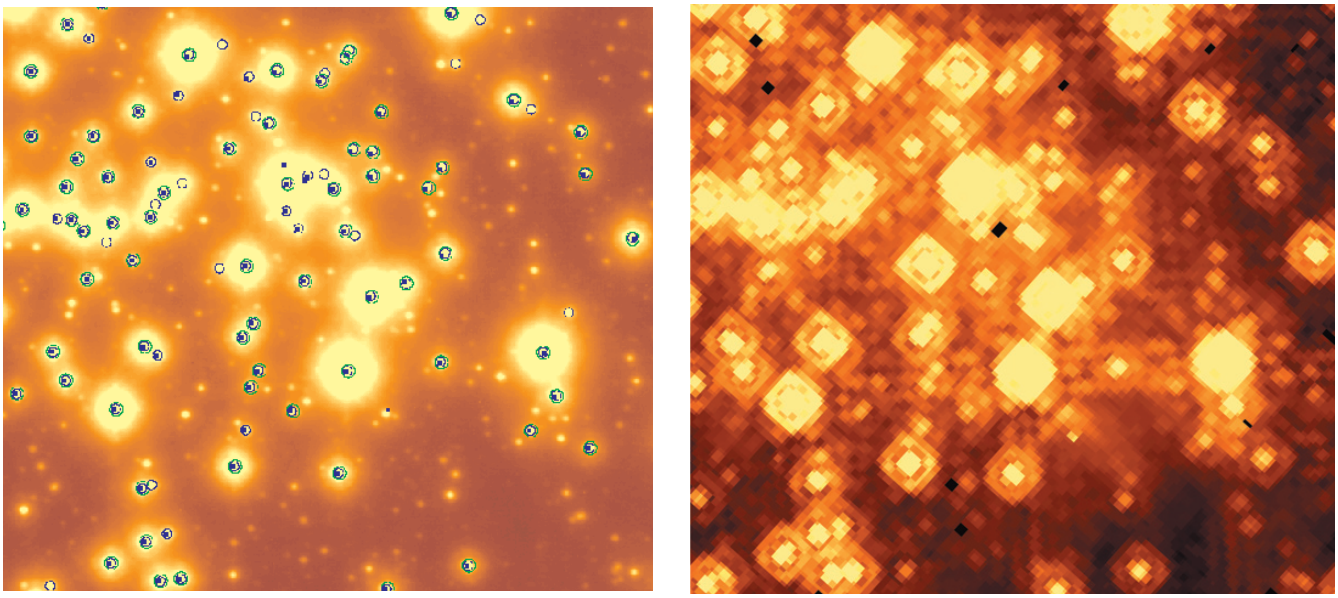

Figure 4: Sources brighter than 15 mag, the Hokupa'a 90% completeness limit, overlaid on the 7 min NACO K-band image (9′ × 9′ FOV, left panel). For comparison, the same area on the NICMOS K-band (F205W) image is shown in the right panel. Blue circles are NACO sources and dots are NICMOS detections in both filters. Green, larger circles are Hokupa'a sources. Several close neighbours of bright sources and equal brightness pairs are exclusively detected in the high resolution NACO data.

have been transformed to the NICMOS system using the colour equations determined by Brandner et al. 2001. A linear change in extinction is observed when moving outwards from the cluster centre. While the innermost 5″ of the cluster population are consistent with a constant reddening of AV = 24.1 mag, the extinction increases with increasing radial distance at radii R > 5″. The observed *H-K* colour as well as the *K*-band magnitude have been corrected for this trend before transformation into stellar masses. A colour cut with 1.35 < $(H\text{-}K)_{corr}$ < 1.77 mag was applied to select Arches main sequence stars from the corrected CMD.

The present-day mass function for stars in the Arches cluster derived from the NACO CMD (Fig. 3) is shown in Figure 5. A power law can easily be fitted to the upper end of the MF for M > 10 $M_{\odot}$, below which the MF appears to become flat. When regarding the entire NACO field, it appears that at this point field contamination sets in, as this flat portion of the MF is very pronounced in MFs created with the above procedure at large distances from the cluster centre. Analysis of Galactic Centre fields in the vicinity of Arches is required to estimate the relative fractions of field and cluster stars in the faint regime. As the combined field of view obtained during Comm 3 does not cover sufficient area at large enough distances from the cluster to perform statistical background subtraction, the MF discussed here focuses on the massive end with M > 10 $M_{\odot}$, where field contamination is negligible.

To eliminate the dependence of binning on the derived MF slope, the starting point of the first mass bin has been shifted by $\delta\log(M/M_{\odot})$ = 0.01 at the chosen bin width of $\Delta\log(M/M_{\odot})$ = 0.1, resulting in ten MFs with consecutive starting points. Averaging the resultant MF slopes yields an MF slope of Γ = –0.91 ± 0.15 for the Arches main sequence, where Salpeter is Γ = –1.35 (Salpeter 1955). Although the NACO LF is more complete, this slope is identical to the slope derived from NICMOS data before (Stolte et al. 2002). This indicates that at the bright end (K < 16 mag, M > 10 $M_{\odot}$), all bins contributing to the LF and MF gain the same fraction of stars, such that the relative fraction of stars in each bin remains the same. Note that we only consider the massive end of the MF, up to K = 16 mag, such that the faint end of the LF, where the largest discrepancy to the NICMOS LF is observed, is not taken into account here, as this would require field subtraction.

This slope is slightly flatter than the average slope of Γ = –1.1 ± 0.3 found in star forming regions in the Milky Way (Massey et al. 1995). A comparably flat slope is seen in the MF of the massive starburst cluster in NGC 3603, which has physical properties similar to Arches, although forming in a much more moderate star-forming environment in the Carina spiral arm. In NGC 3603, the MF slope is found to be Γ = –0.7 in the mass range 1$M_{\odot}$ < M < 30 $M_{\odot}$ (Eisenhauer et al. 1998), close to the Arches MF slope. The flat slope indicates that the Arches cluster was either very efficient in forming massive stars, or that dynamical mass segregation has led to the ejection of a significant number of intermediate-mass stars. If the cluster is mass segregated (either due to primordial or due to dynamical processes), this should be particularly pronounced in the cluster centre.

The cluster centre MF is shown in Figure 5 (right). Only stars within the innermost 5″ of the cluster centre are included. The binning width was now chosen to be $\Delta\log(M/M_{\odot})$ = 0.2 for statistical reasons. Again, only the bright end of the MF was fitted for comparison purposes. The average slope derived for the cluster centre with the same method as described above is Γ = –0.6 ± 0.2, flatter than the slope for the entire cluster. This is consistent with massive star cluster formation scenarios, where primordial or rapid dynamical segregation causes massive stars to end up in the cluster centre, while a larger fraction of low-mass stars is found in the outskirts.

Although the entire mass range in the cluster centre appears to be consistent with a very flat MF ($\Gamma \sim 0$) down to $\log(M/M_{\odot}) \sim 0.5$, M = 3 $M_{\odot}$, where the *K*-band LF is more than 75% complete (derived from stars recovered in both *H* and *K*), it is currently not clear how the interplay of incompleteness correction and field contamination will alter the shape of the MF for masses below 10 $M_{\odot}$. Neighbouring Galactic Centre fields and thorough incompleteness testing will be required to obtain a meaningful slope in the cluster centre down to the low-mass regime.

7. Outlook

Velocity studies of the bright cluster stars in the vicinity of Arches are necessary to draw final conclusions on the formation scenario. Stars dynamically ejected during interaction processes should obtain large velocities directed away from the cluster centre. Such a velocity study can yield new insights into the cluster dynamics as well as for-

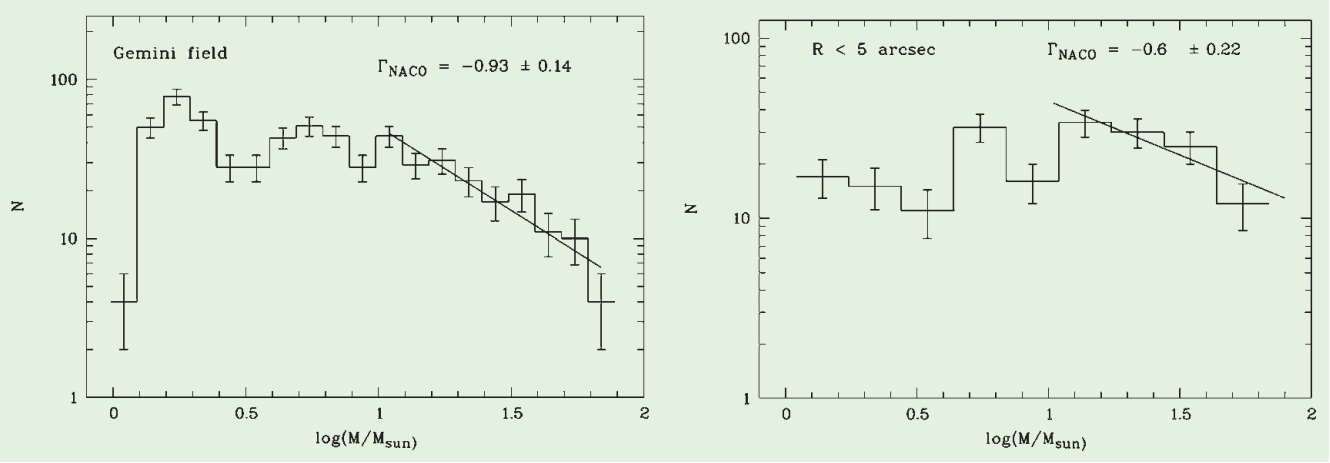

Figure 5: Mass Function of the Arches cluster. Left panel: The area within the Gemini FOV has been selected, such that the MF corresponds to the CMD displayed in Figure 3. A linear change in extinction over the field has been corrected, and a colour cut of 1.35 < H-K < 1.77 mag has been applied to the corrected CMD to select Arches main-sequence stars. The Arches main sequence can clearly be identified down to 18.3 mag in K-band, or 2.5 $M_{\odot}$ (logM/$M_{\odot}$ = 0.4), beyond which the bulge population dominates the CMD. Right panel: The mass function of Arches cluster centre stars observed with NACO. Stars within R < 5″ are included. A weighted least-squares fit has been performed on data points above 10 $M_{\odot}$. The MF in the cluster centre appears flatter than the integrated MF, indicating mass segregation.

mer cluster membership of ejected stars. High-resolution NIR spectrographs such as CRIRES expected to go into operation in the next years have the capability to overcome the huge line of sight obscuration towards the Galactic Centre. The determination of spectral types with SINFONI/SPIFFI allows one to disentangle the cluster members from the dense background population, thereby yielding accurate estimates on the field star contamination when deriving mass functions. With these prospects in mind, spectroscopic observations may shed light on the unsolved questions of massive star formation in a dense environment.

8. Conclusions

NAOS-CONICA data of the dense stellar field in the Arches cluster centre yield significantly better spatial resolution than NICMOS on HST. About 50% more stars are resolved in the cluster centre down to the same magnitude limit. The luminosity functions reveal that each magnitude interval up to the brightest stars was affected by crowding losses before. The NACO observations of the densest cluster region within R < 5″ are 75% complete down to H = 19.4 mag and K = 17.7 mag or ~ 3 $M_{\odot}$, while HST/NICMOS and Gemini/Hokupa'a observations were limited to ~10–20 $M_{\odot}$ in the immediate cluster centre. While a lower Strehl ratio is responsible for the lower performance in the Hokupa'a data, the NICMOS resolution is limited by the smaller HST mirror and correspondingly larger diffraction limit. As we have shown, even moderate AO performance using faint visual reference sources (V = 16 mag) now achieves higher spatial resolution from the ground while at the same time exploiting the light collecting power and sensitivity of 8-m-class telescopes. Thus, a much more complete census of stellar populations in dense fields in our own Galaxy as well as in nearby resolved galactic systems is possible with ground-based AO instruments such as NAOS-CONICA.

References

Blum, R. D., Schaerer, D., Pasquali, A., et al. 2001, *AJ*, **122**, 1875.

Brandner, W., Grebel, E. K., Barbá, R. H., et al. 2001, *AJ*, **122**, 858.

Brandner, W., Rousset, G., Lenzen, R., Hubin, N. et al. 2002, *The Messenger* No. **107**, 1.

Cotera, A.S., Erickson, E.F., Colgan, S.W.J., Simpson. J.P., Allen, D.A., & Burton, M.G., 1996, *ApJ*, **461**, 750.

Devillard, N. 1997, *The Messenger* No **87**, 19.

Eisenhauer, F., Quirrenbach, A., Zinnecker, H., Genzel, R. 1998, *ApJ*, **498**, 278.

Figer, D.F., Najarro, F., Gilmore, D., et al. 2002, *ApJ*, **581**, 258.

Figer, D.F., Kim, S.S., Morris, M., et al. 1999, *ApJ*, **525,** 750.

Lejeune, T., & Schaerer, D. 2001, *A&A*, **366**, 538.

Lenzen, R., Hoffmann, R. et al. 1998, *SPIE* **3354**, 606.

Massey, P., Johnson, K.E., Degioia-Eastwood, K. 1995, *ApJ*, **454**, 151.

Rieke, G.H., & Lebofsky, M.J. 1985, *ApJ*, **288**, 618.

Rousset, G., Lacombe, F. et al. 2002, *SPIE* **4007**, 72.

Salpeter, E.E. 1955, *ApJ*, **121**, 161.

Scalo, J.M. 1998, in *ASP Conf. Ser.*, Vol. **142**, The stellar initial mass function, 201.

Schoedel, R., Ott, T., Genzel, R. et al. 2002, *Nature* **419**, 694.

Stetson, P.B. 1987, *PASP*, **99**, 191.

Stolte, A., Grebel, E.K., Brandner, W., Figer, D.F., 2002, *A&A*, **394**, 462.

Tessier, E., Bouvier, J., Beuzit, J.-L., Brandner, W. 1994, *The Messenger* No. **78**, 35.

Early Galactic Chemical Evolution with UVES

M. PETTINI, Institute of Astronomy, Cambridge, UK

The UVES instrument on the ESO VLT2 telescope has now been providing high-resolution spectra of faint stars and galaxies for nearly three years. European astronomers have taken advantage of this new facility to conduct extensive and accurate studies of the first stellar generations of our Galaxy, and to probe the chemical composition of gas in the high-redshift universe. In November of last year, a workshop on the theme "Early Galactic Chemical Evolution with UVES" was held at the ESO headquarters in Garching. Attended by more than 50 stellar and extragalactic astronomers, the workshop served as a focus to bring together scientists interested in the general theme of how the chemical enrichment of galaxies progressed over the cosmic ages, from the Big Bang to the present time. The meeting proved to be a valuable opportunity to exchange ideas, assess progress to date, and to chart fu-